

The public reporting burden for this collection of information is estimated to average 1 hour per response, including the time for reviewing instructions, searching existing data sources, gathering and maintaining the data needed, and completing and reviewing the collection of information. Send comments regarding this burden estimate or any other aspect of this collection of information, including suggestions for reducing this burden, to Washington Headquarters Services, Directorate for Information Operations and Reports, 1215 Jefferson Davis Highway, Suite 1204, Arlington VA, 22202-4302. Respondents should be aware that notwithstanding any other provision of law, no person shall be subject to any penalty for failing to comply with a collection of information if it does not display a currently valid OMB control number.
PLEASE DO NOT RETURN YOUR FORM TO THE ABOVE ADDRESS.

1. REPORT DATE (DD-MM-YYYY) 03-02-2023	2. REPORT TYPE Final Report	3. DATES COVERED (From - To) 4-Oct-2018 - 3-Oct-2022
---	--------------------------------	---

4. TITLE AND SUBTITLE Final Report: Study of PIN Junctions in GaAsSb Nanowires on Si for the Next Generation Infrared Photodetectors	5a. CONTRACT NUMBER W911NF-19-1-0002
	5b. GRANT NUMBER
	5c. PROGRAM ELEMENT NUMBER 106012

6. AUTHORS	5d. PROJECT NUMBER
	5e. TASK NUMBER
	5f. WORK UNIT NUMBER

7. PERFORMING ORGANIZATION NAMES AND ADDRESSES North Carolina A&T State University 1601 East Market Street Greensboro, NC 27411 -0001	8. PERFORMING ORGANIZATION REPORT NUMBER
--	--

9. SPONSORING/MONITORING AGENCY NAME(S) AND ADDRESS (ES) U.S. Army Research Office P.O. Box 12211 Research Triangle Park, NC 27709-2211	10. SPONSOR/MONITOR'S ACRONYM(S) ARO
	11. SPONSOR/MONITOR'S REPORT NUMBER(S) 72457-RT-REP.25

12. DISTRIBUTION AVAILABILITY STATEMENT 2 Approved for public release; distribution is unlimited

13. SUPPLEMENTARY NOTES The views, opinions and/or findings contained in this report are those of the author(s) and should not be construed as an official Department of the Army position, policy or decision, unless so designated by other documentation.

14. ABSTRACT

15. SUBJECT TERMS

16. SECURITY CLASSIFICATION OF:			17. LIMITATION OF ABSTRACT UU	15. NUMBER OF PAGES	19a. NAME OF RESPONSIBLE PERSON Shanthi Iyer
a. REPORT UU	b. ABSTRACT UU	c. THIS PAGE UU			19b. TELEPHONE NUMBER 336-285-3710

RPPR
as of 09-Feb-2023

Agency Code:

Proposal Number:

Agreement Number:

Organization:

Address: , ,

Country:

DUNS Number:

EIN:

Date Received:

Report Date:

for Period Beginning and Ending

Title:

Begin Performance Period:

End Performance Period:

Report Term: -

Submitted By:

Email:

Phone:

Distribution Statement: -

STEM Degrees:

STEM Participants:

Major Goals:

Accomplishments:

Training Opportunities:

Results Dissemination:

Plans Next Period:

Honors and Awards:

Protocol Activity Status:

Technology Transfer:

I certify that the information in the report is complete and accurate:

Signature:

Signature Date:

Abstract

A comprehensive investigation of p-i-n (PIN) structured GaAsSb nanowire (NW) growths by molecular beam epitaxy and high performance near infrared-based photodetectors (PD) of axial and core-shell (CS) architectures are presented. GaAsSb NW exhibited space charge limited conduction mechanism. In-situ annealed NWs revealed significant reduction in the trap density from 10^{16} cm^{-3} in as-grown NWs to a low level of $7 * 10^{14} \text{ cm}^{-3}$ and confining wider trap energy distribution to a narrow distribution of 0.12 eV. Te-doping assessment in NWs was successfully accomplished using GaTe captive source and surface analytical tools XPS/UPS and C-AFM/SKPM. A Schottky barrier photodetector was demonstrated using Te-doped ensemble NWs with a broad spectral range and a longer wavelength cut-off at $\sim 1.2 \mu\text{m}$. These photodetectors exhibited high responsivity in the range of 580 – 620 A/W and detectivity of $1.2 - 3.8 \times 10^{12}$ Jones. Our study of ultrafast carrier transport and recombination dynamics in Te-doped GaAsSb shows a carrier recombination lifetime of $147 \pm 3 \text{ ps}$ with a fast rise time of $\sim 2\text{ps}$. We also show that the ex-situ atomic layer deposited Al_2O_3 layer is not an effective GaAsSb NW passivator.

These studies were then used to fabricate high-performance conventional n-i-p GaAsSb C-S configured NWs on $\langle 111 \rangle$ Si with responsivity and detectivity of 190 A/W and 1.1×10^{14} Jones, respectively, at -1 V bias and $1.1 \mu\text{m}$. By tailoring the intrinsic region shell thickness grown on top of the core- Te- doped GaAsSb and surrounded by shell Be- doped GaAsSb, a novel hybrid axial C-S n-i-p GaAsSb NW structure enabled enhanced light absorption volume and extension of the wavelength region of operation to $1.5 \mu\text{m}$ with responsivity and detectivity of 18 A/W and 1.1×10^{13} Jones, respectively at RT. In addition, a high-quality C-S junction in the hybrid structure was demonstrated by a high rectification ratio of the diode, suppression of low-frequency noise, lack of 1/f noise, and a low corner frequency of $\sim 2.5 \text{ Hz}$. Axial configured p-i-n NWs on $\langle 111 \rangle$ Si with a responsivity of $\sim 120 \text{ A/W}$, a detectivity of $\sim 1.1 \times 10^{13}$ Jones at -3V reverse bias, with cut-off wavelength at $1.1 \mu\text{m}$ were also successfully realized by appropriately mitigating the effects of the Ga droplet reservoir effect, and the radial overgrowth issues.

Finally, this work formed an excellent training ground for students in state-of-the-art research at the nanoscale. It resulted in several journal publications with students as the principal author.

1st Reporting Period

A Study on the Effects of Gallium Droplet Consumption and Post-Growth Annealing on Te-Doped GaAs Nanowire Properties grown by Self-Catalyzed Molecular Beam Epitaxy

In this work, the effects of As flux used during Ga seed droplet consumption and the post-growth annealing on the optical, electrical, and microstructural properties of self-catalyzed molecular beam epitaxially grown Te-doped GaAs nanowires (NWs) have been investigated using a variety of characterization techniques. NWs using the same amount of As flux for growth of the seed droplet consumption demonstrated reduced density of stacking faults at the NW tip with ~ 4 -fold enhancement in the 4K PL intensity and increased single nanowire photocurrent over their higher As flux droplet consumption counterparts. Post-growth annealed NWs exhibited an additional low-energy PL peak at 1.31 eV that significantly reduced the overall PL intensity. The origin of this lower energy peak is assigned to a photocarrier transition from the conduction band to the annealing-assisted Te-induced complex acceptor state ($\text{Te}_{\text{As}}\text{V}_{\text{Ga}}^-$). In addition, post-growth

annealing demonstrated a detrimental impact on the electrical properties of the Te-doped GaAs NWs as revealed by suppressed single nanowire (SNW) and ensemble NW photocurrent with a consequently enhanced low-frequency noise level compared to as-grown doped NWs. This work demonstrates that each parameter in the growth space must be carefully examined to successfully grow self-catalyzed Te-doped NWs of high quality and is not a simple extension of the growth of corresponding intrinsic NWs.

-This work has been published in *Catalysts* 12, 451 (2022). <https://doi.org/10.3390/catal12050451> and also a part of *Shisir Devkota's Ph.D. Dissertation*

Space charge limited conduction mechanism in GaAsSb nanowires and the effect of in-situ annealing in ultra-high vacuum

In this work, the first observation of the space charge limited conduction mechanism (SCLC) in GaAsSb nanowires (NWs) grown by Ga-assisted molecular beam epitaxial technique and the effect of ultrahigh vacuum in-situ annealing have been investigated. The low onset voltage of the SCLC in the NW configuration has been advantageously exploited to extract trap density and trap **energy** distribution in the band gap of this material system, using simple temperature-dependent current-voltage measurements in both the ensemble and single nanowires. In-situ annealing in an ultra-high vacuum revealed a significant reduction in the trap density from 10^{16} cm^{-3} in as-grown NWs to a low level of $7 * 10^{14} \text{ cm}^{-3}$ and confining wider trap energy distribution to a narrow distribution of 0.12 eV. A comparison of the current conduction mechanism in the respective single nanowires using conductive atomic force microscopy (C-AFM) further confirms the SCLC mechanism identified in the GaAsSb ensemble device to be intrinsic. Higher current observed in current mapping by C-AFM, increased 4K photoluminescence (PL) intensity along with reduced full-width half maxima and more symmetric PL spectra, reduced asymmetrical broadening, and increased TO/LO mode in room temperature Raman spectra for in-situ annealed NWs again attest to effective annihilation of traps leading to the improved optical quality of NWs compared to as-grown NWs. Hence, the I-V-T analysis of the SCLC mechanism has been demonstrated to be a simple approach to obtaining information on growth-induced traps in the NWs.

-This work has been published in *Nanotechnology*, 31, 025205 (2020), <https://doi.org/10.1088/1361-6528/ab47aa>.

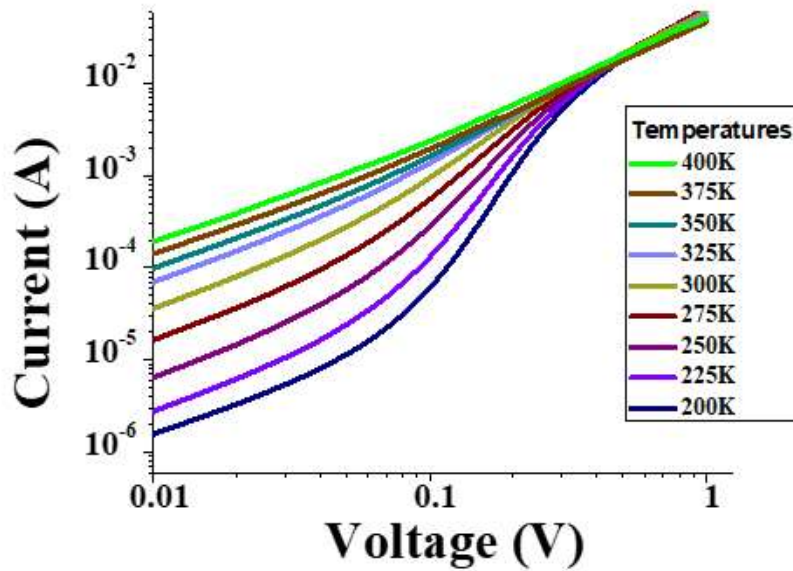


Figure: Temperature dependence of log I-log V characteristics of in-situ annealed NW ensemble device.

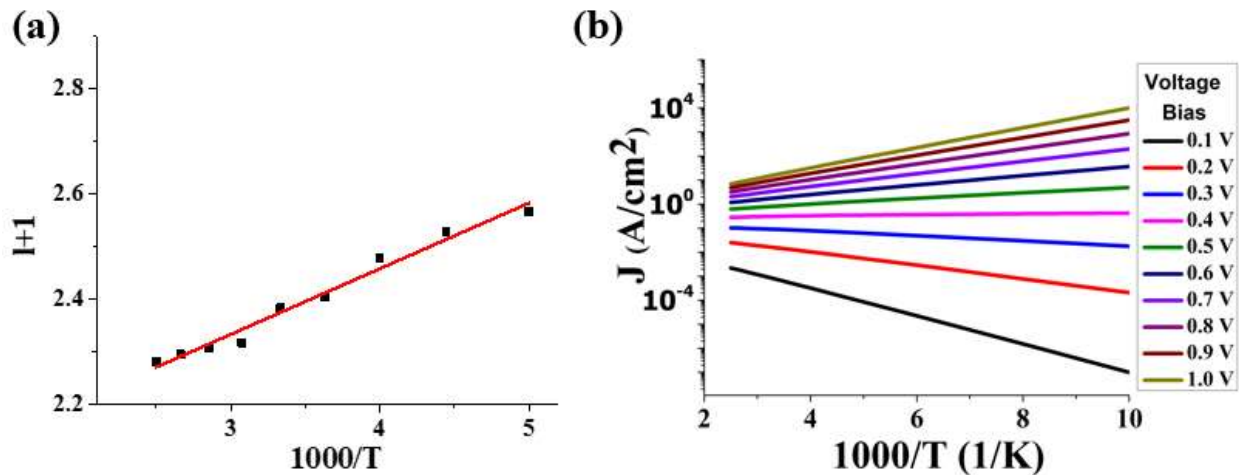


Figure: Log J vs. (1/T) plot at different voltages shows temperature invariance characteristics at $V_c = 0.4$ V.

2nd Reporting Period

Doping Assessment

We report the first study on the Te-doping assessment in Te-doped GaAsSb nanowires (NWs) using X-ray photoelectron spectroscopy (XPS), ultraviolet photoelectron spectroscopy (UPS), conductive-atomic force microscopy (C-AFM), and scanning Kelvin probe microscopy (SKPM). The Te-dopant concentration and electron density determined from all the techniques were in the range of $1-3 \times 10^{19} \text{ cm}^{-3}$ showing the reliability of these measurement techniques for uniformly

doped NWs. Thus, the surface analytical tools XPS/UPS and C-AFM/SKPM, devoid of any sample preparation, are found to be powerful characterization techniques for analyzing the dopant incorporation and carrier density in homogeneously doped NWs.

-This work has been published in *Scientific Reports*, 11, 8329 (14 pages) (2021). <https://doi.org/10.1038/s41598-021-87825-4>. This also formed a part of Priyanka Ramaswamy's Ph.D. dissertation.

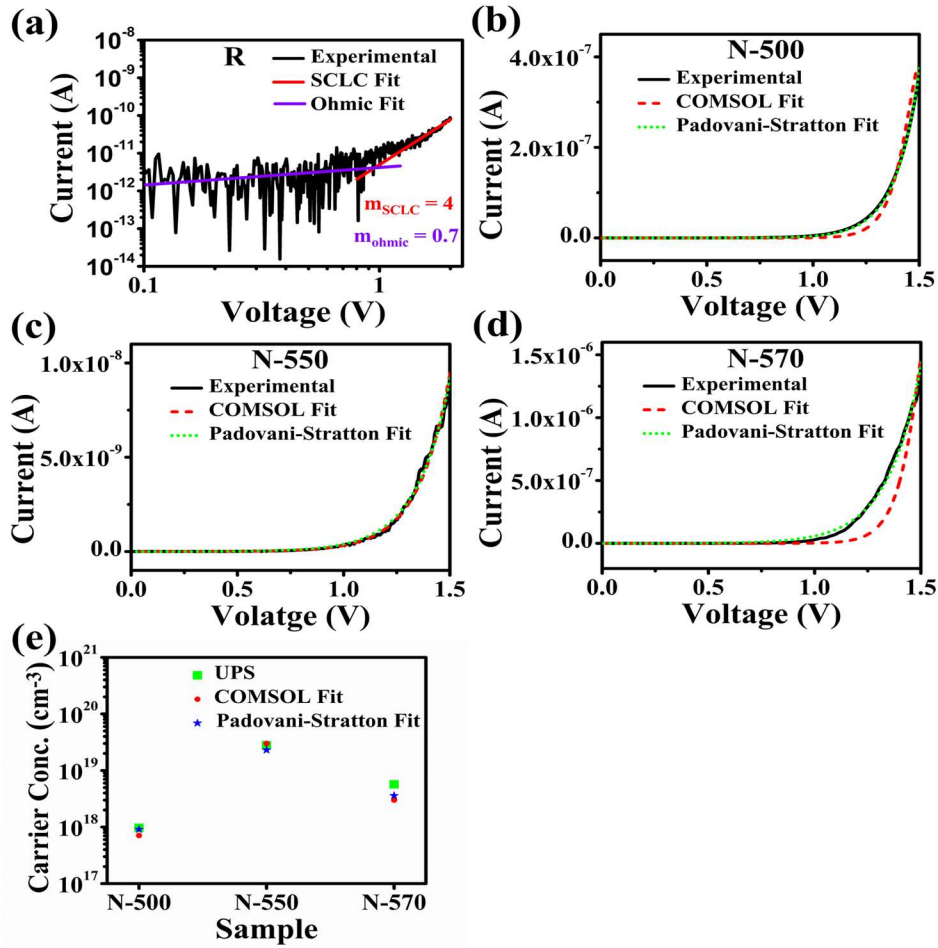


Figure: (a) Log-log I-V characteristic of R sample exhibiting linear and power dependence, (b-d) experimental I-V dark, simulated COMSOL fit, and Schottky diode fitting of dark I-V characteristics of (b) N-500, (c) N-550, and (d) N-570 samples, and (e) carrier concentration of N-500, N-550, and N-570 samples extracted from UPS, COMSOL fit, and Padovani-Stratton fit.

Te Doping and Schottky Barrier Photodetector

A comprehensive investigation of the effect of gallium telluride (GaTe) cell temperature variation (T_{GaTe}) on the morphological, optical, and electrical properties of doped-GaAsSb nanowires (NWs) grown by Ga-assisted molecular beam epitaxy (MBE) was carried out. These

studies led to an optimum doping temperature of 550 °C for the growth of tellurium (Te)-doped GaAsSb NWs with the best optoelectronic and structural properties. Te incorporation resulted in a decrease in the aspect ratio of the NWs, causing an increase in the Raman LO/TO vibrational mode intensity ratio, large PL emission with an exponential decay tail on the high energy side, promoting tunnel-assisted current conduction in ensemble NWs and significant photocurrent enhancement in the single nanowire. A Schottky barrier photodetector was demonstrated using Te-doped ensemble NWs with broad spectral range and a longer wavelength cut-off at $\sim 1.2 \mu\text{m}$. These photodetectors exhibited responsivity in the range of 580 – 620 A/W and detectivity of $1.2 - 3.8 \times 10^{12}$ Jones.

-This work has been published in *Nanotechnology*, 31, 505203(10pp) (2020) <https://doi.org/10.1088/1361-6528/abb506> . This also formed part of *Shisir Devkota's Ph.D. Dissertation*

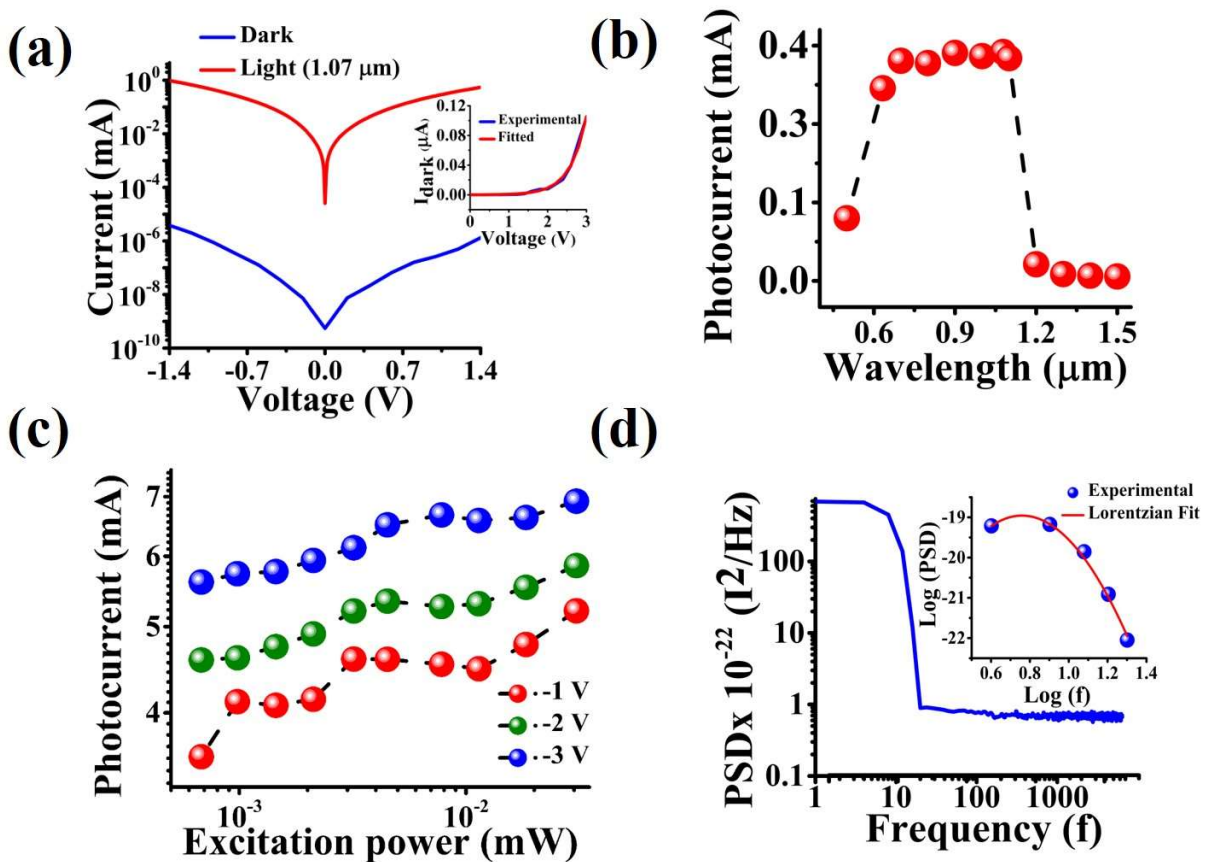


Figure: N-GaAsSb NW ensemble PD device: (a) dark and photocurrent (at $\sim 1.07 \mu\text{m}$) superimposed in semi-log scale, and the inset shows the Schottky diode fitting to calculate tunneling parameter (E_{00}), (b) spectral response, (c) excitation power dependent photocurrent at -1 V, -2 V and -3 V bias for 0.63 μm laser excitation, (d) dark current noise spectra (S_I) at the reverse applied bias of 1 V, and the inset shows the Lorentzian fit of dark current noise after the roll-off.

Lumerical Finite-Difference Time-Domain modeling of Absorption Characteristics

Lumerical Finite-Difference Time-Domain modeling has been used to simulate the absorption characteristics of P-I-N axial and core-shell gallium arsenide antimonide (GaAsSb) nanowires. A Kramer-Kronig's analysis was used to determine the change in refractive index and extinction coefficient for a GaAsSb thin film of different doping concentrations, which was then used to simulate the absorption characteristics in the nanowire configuration. It was found that increasing n-type doping decreases the absorption percentage when the n- segment forms the outermost part (shell) of the nanowire configuration. The optimal absorbance spectra for GaAsSb nanowires for arrays were determined by varying nanowire diameter, pitch length, and array configuration. Also, other absorption boosting techniques, such as using aluminum gallium arsenide (AlGaAs) as a passivation material and coating a silicon dioxide (SiO₂) shell on GaAsSb nanowires, were employed. Results show that nanowires with a diameter ranging from 100 nm - 150 nm with a pitch length of 400 nm provide the optimal absorbance spectra according to simulations for axial and core-shell configurations. Also, including a SiO₂ shell in the axial nanowire boosted absorption in the near-infrared region by approximately 30 %. Results show that Lumerical FDTD can be used as a powerful simulation tool for the optical simulation of nanowire arrays for device application while reducing experimental iterations.

-This was the focus of *Kendall Dawkins* Master's thesis.

3rd and Final Extension Reporting Period

MBE-grown hybrid axial core-shell n-i-p GaAsSb heterojunction ensemble nanowires based near infrared photodetectors up to 1.5 μm

In this paper, a high performance self-assisted molecular beam epitaxy (MBE) grown conventional core-shell (C-S) n-i-p GaAsSb nanowires (NWs) and novel hybrid axial C-S n-i-p GaAsSb ensemble NWs based near-infrared photodetector (NIRPD) on non-patterned Si substrate are demonstrated. The conventional room temperature (RT) C-S n-i-p GaAsSb NW with a high responsivity of 190 A/W and a higher detectivity of 1.1×10^{14} Jones at -1V bias at the wavelength of 1.1 μm is reported by optimizing the intrinsic region thickness and appropriately compensating the intrinsic p-type behavior with n-dopant Te. Furthermore, hybrid axial C-S n-i-p GaAsSb has been bandgap engineered for the wavelength up to 1.5 μm exhibiting responsivity of 18 A/W and detectivity of 1.1×10^{13} Jones operating at RT. In this hybrid design, we have combined both axial and radial intrinsic (i-) segments of different Sb% compositions to enhance the photoabsorption in the NIR region, hence the photogenerated current, and also the high bandgap axial *i- region helps to suppress the trap-assisted tunneling mechanism, which is found to be advantageous over conventional C-S NW architectures*. In addition, high rectification ratio from current-voltage measurements (I-V), suppression of low frequency noise, lack of 1/f noise, a low corner frequency of ~2.5 Hz beyond which presence of only frequency-independent white noise from low-frequency noise measurements (LFN), and bias- and frequency- dependent capacitance-voltage (C-V) measurements suggest the formation of high-quality C-S junction in the hybrid structure. Thus,

our findings reveal that the hybrid axial C-S NW architecture provides the flexibility of 3D design, which offers the unprecedented prospect for expanding IRPD and other next-generation optoelectronic device applications.

-This work has been published in *Crystal Growth and Design* 22 (10) 6004-6014. DOI: 10.1021/acs.cgd.2c00652. This is also a major portion of Priyanka Ramaswamy's Ph.D. dissertation.

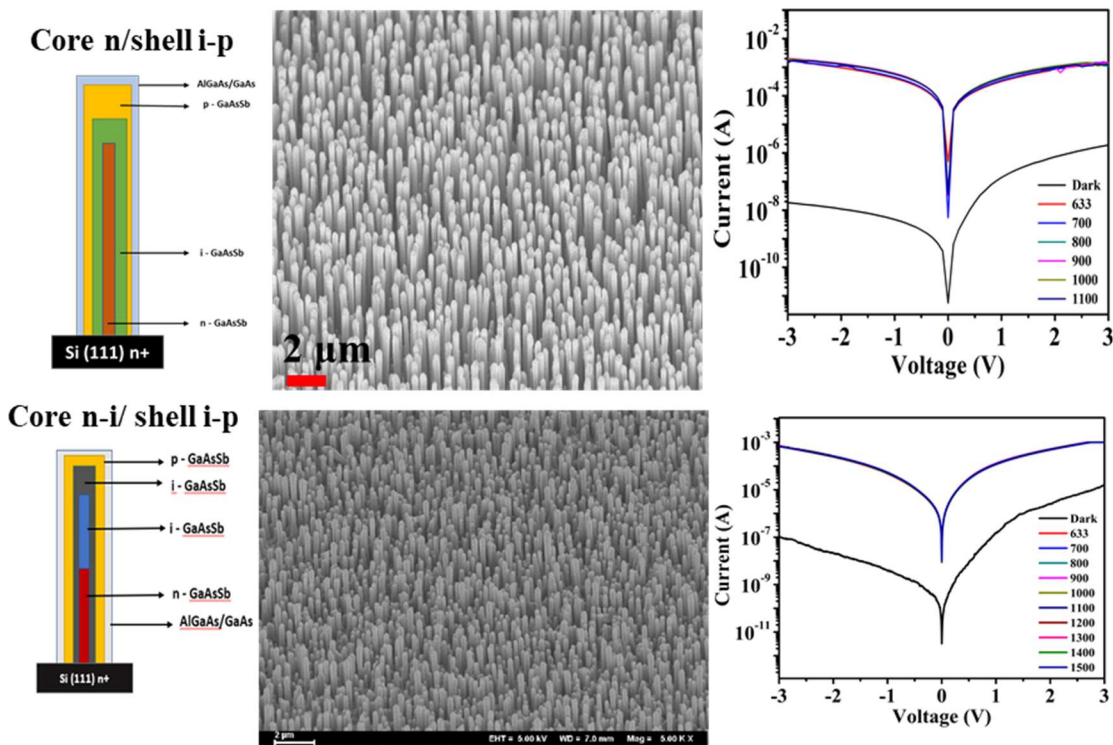


Figure: Schematic diagram of core n/shell i-p (top) and core n-i/shell i-p (bottom) GaAsSb NWs with the respective SEM images and wavelength-dependent I-V characteristics.

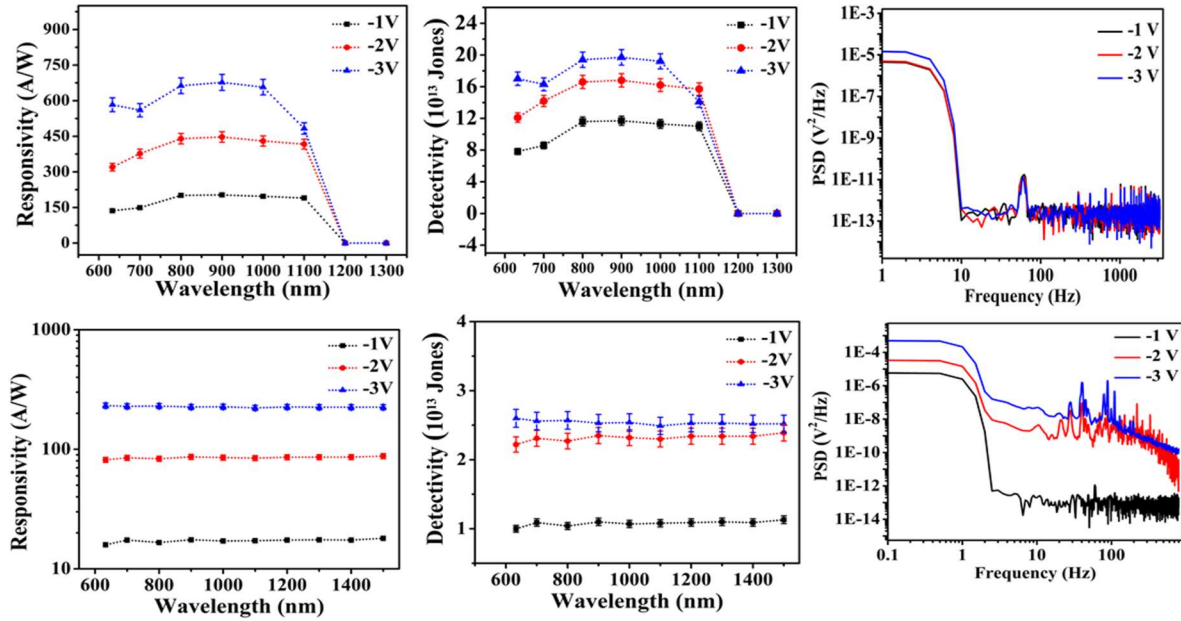


Figure: Responsivity, detectivity and LFN characteristics of core n/shell i-p (top) and core n-i/shell i-p (bottom) GaAsSb NW.

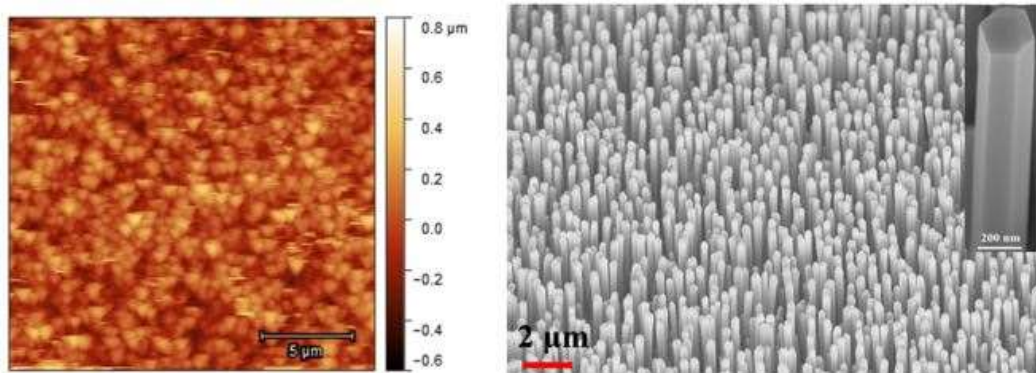


Figure: AFM and SEM images of MBE-grown core-shell n-i-p GaAsSb high performance nanowires

Heterostructure axial GaAsSb ensemble near-infrared p-i-n based axial configured nanowire photodetectors

In this work, we present a systematic design of growth experiments and subsequent characterization of self-catalyzed molecular beam epitaxially grown GaAsSb heterostructure axial p-i-n nanowires (NWs) on p-Si <111> for the ensemble photodetector (PD) application in the near-infrared (NIR) region. Diverse growth methods have been explored to gain a better insight into mitigating several growth challenges by systematically studying their impact on the NW electrical and optical properties to realize a high-quality p-i-n heterostructure. The successful growth approaches are Te-dopant compensation to suppress the p-type nature of intrinsic GaAsSb segment, growth interruption for strain relaxation at the interface, decreased substrate temperature

to enhance supersaturation and minimize the reservoir effect, higher bandgap compositions of the n-segment of the heterostructure relative to the intrinsic region for boosting the absorption, and the high-temperature ultra-high vacuum in-situ annealing to reduce the parasitic radial overgrowth. The efficacy of these methods is supported by enhanced photoluminescence (PL) emission, suppressed dark current in the heterostructure p-i-n NWs accompanied by increased rectification ratio, photosensitivity, and a reduced low-frequency noise level. The PD fabricated utilizing the optimized GaAsSb axial p-i-n NWs exhibited the longer wavelength cut-off at $\sim 1.1 \mu\text{m}$ with a significantly higher responsivity of $\sim 120 \text{ A/W}$ (@-3 V bias) and a detectivity of 1.1×10^{13} Jones operating at room temperature. Frequency and the bias independent capacitance in the pico-Farad (pF) range and substantially lower noise level at the reverse biased condition, show the prospects of p-i-n GaAsSb NWs PD for high-speed optoelectronic applications.

-This work is under review in *Nanotechnology* and part of *Shisir Devkota's Ph.D. Dissertation.*

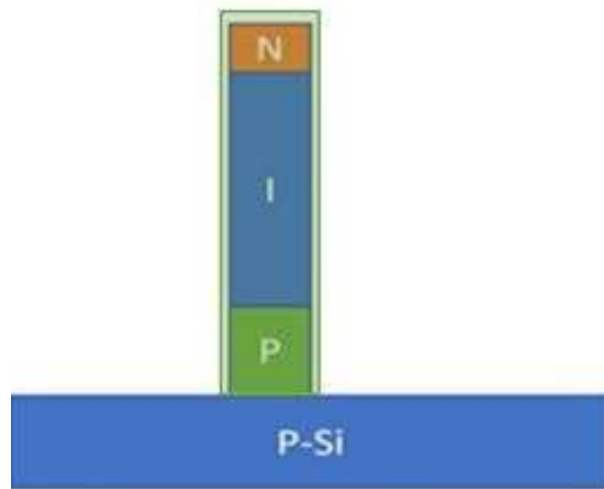


Figure: Schematic of p-i-n NW axial configuration.

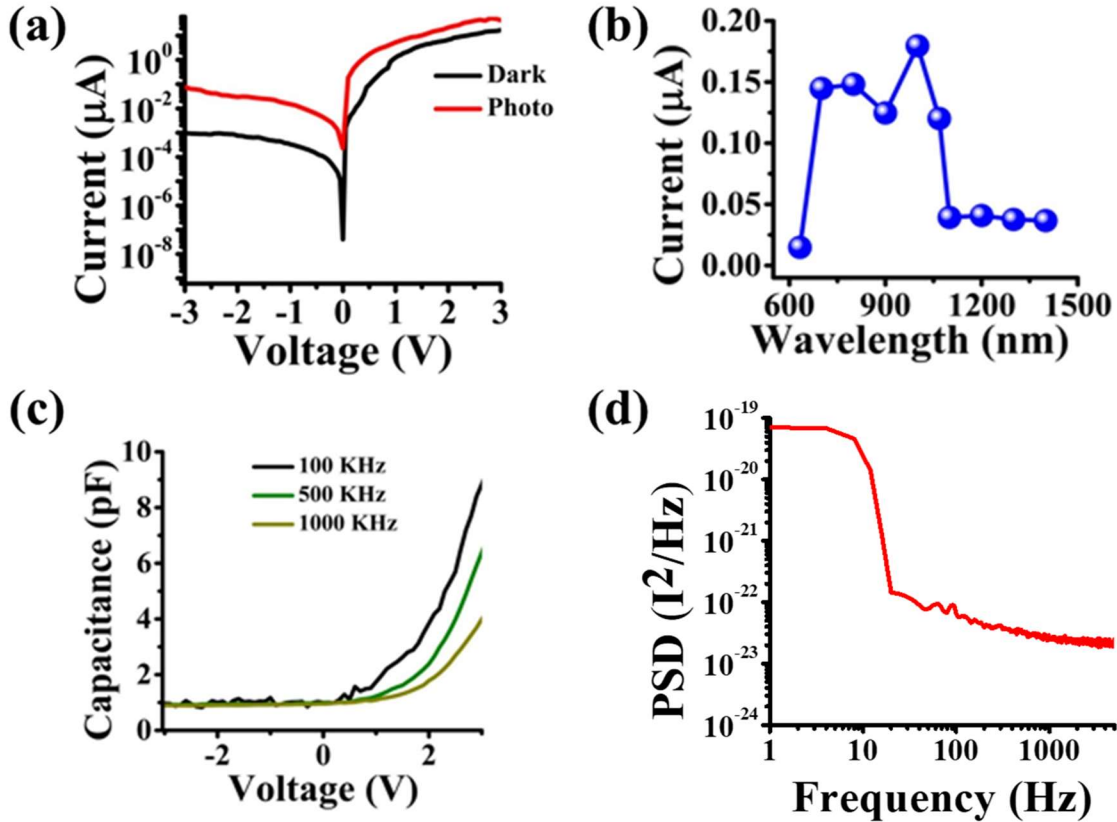


Figure: (a) Superimposed dark and photocurrent, (b) spectral response (@-3 V), C-V measurements at different frequencies, and (d) LFN spectroscopy (@-3 V) of the ensemble axial heterostructure p-i-n NW photodetectors.

Passivation efficacy study of Al₂O₃ dielectric on self-catalyzed molecular beam epitaxially grown GaAs_{1-x}Sb_x nanowires

The effect of sulfur treatment and Al₂O₃ passivation using thermal ALD ex-situ deposition on self-catalyzed GaAsSb NWs using XPS, PL spectroscopy, and Raman spectroscopy were successfully studied. The 4K-PL spectra revealed a significant drop in PL intensity (~ 10-fold) for Al₂O₃ passivated NWs compared to as-grown, irrespective of prior sulfur treatment. The XPS spectral analysis indicated that precleaning with sulfur treatment before Al₂O₃ ALD deposition effectively removed III-V native oxides formed on the NW surface, thus ruling out the effect of native oxides on optical degradation. Further, the Raman characterization observed significant redshifts, peak broadening, and asymmetry for Al₂O₃ passivated NWs when compared to as-grown NWs, suggesting the presence of point defects on Al₂O₃ ALD deposition. Hence, the 4K-PL optical degradation observed in both sulfur-treated and untreated Al₂O₃ passivated NWs samples suggests non-radiative recombination centers arising from complex NW/dielectric interface formation to be the main contributing factor. Reporting of similar PL degradation in GaAs NWs, while enhanced PL intensity in In-based NWs [23] allows us to speculate that non-radiative recombination centers arising from the Al₂O₃/NW interface states are peculiar to Ga-based III-V NWs only, and surface

faceting in GaAsSb NWs may also enhance this contribution. Thus, ALD deposited Al₂O₃ layer is not a good choice for the passivation layer for GaAsSb NWs.

-This work has been published in *Nanotechnology*, 31, 025205 (8pp)_(2022) <https://doi.org/10.1088/1361-6528/ac69f8>.

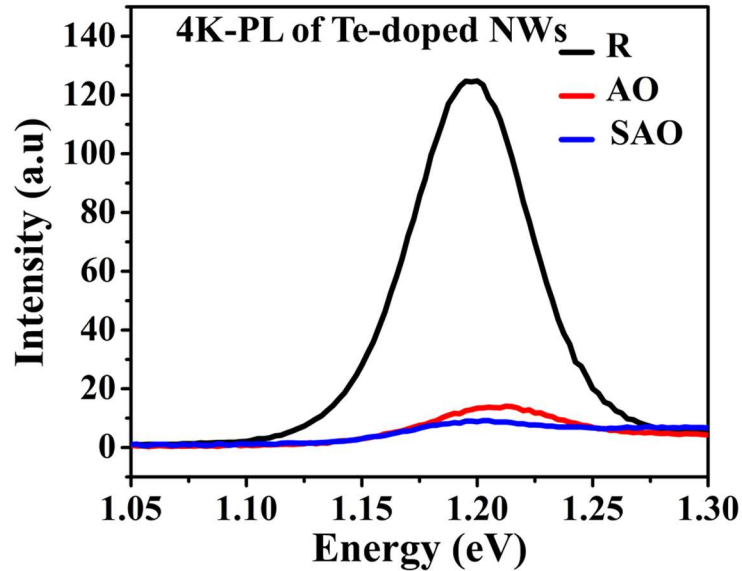


Figure: 4K-PL comparison of Te-doped GaAsSb: Reference [®], as-grown with ex-situ Al₂O₃ passivation layer (AO), and sulfur-treated passivated Al₂O₃ (SAO) samples.

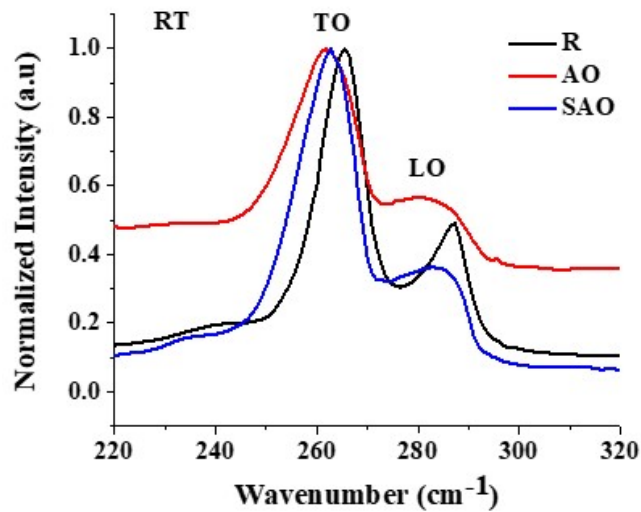


Figure: Normalized RT Raman spectra comparison of R, AO, and SAO samples.

Revealing Charge Carrier Dynamics and Transport in Te-Doped GaAsSb and GaAsSbN Nanowires by Correlating Ultrafast Terahertz Spectroscopy and Optoelectronic Characterization

It is established that a small amount of nitrogen (N) incorporation in III-V semiconductor NWs can effectively redshift their wavelength of operation and tailor their electronic properties for specific applications. However, understanding the impact of N incorporation on non-equilibrium charge carrier dynamics and transport in semiconducting NWs is critical in achieving efficient semiconducting NW devices. In this work, ultrafast optical pump-terahertz probe spectroscopy has been used to study non-equilibrium carrier dynamics and transport in Te-doped GaAsSb and dilute nitride GaAsSbN NWs, with the goal of correlating these results with the electrical characterization of their equilibrium photo-response under bias and low-frequency noise characteristics. Nitrogen incorporation in GaAsSb NWs led to a significant increase in the carrier scattering rate, resulting in a severe reduction in carrier mobility. Carrier recombination lifetimes of 33 ± 1 picoseconds (ps) and 147 ± 3 ps in GaAsSbN and GaAsSb NWs, respectively, were measured. The reduction in the carrier lifetime and photoinduced optical conductivities are due to N-induced defects, leading to deterioration in the electrical and optical characteristics of dilute nitride NWs relative to the non-nitride NWs. Finally, we observed a very fast rise time of ~ 2 ps for both NW materials, directly impacting their potential use as high-speed photodetectors.

-This work has been published in *Nanotechnology*, 33, 425702 (8 pp).DOI: [10.1088/1361-6528/ac7d61](https://doi.org/10.1088/1361-6528/ac7d61)

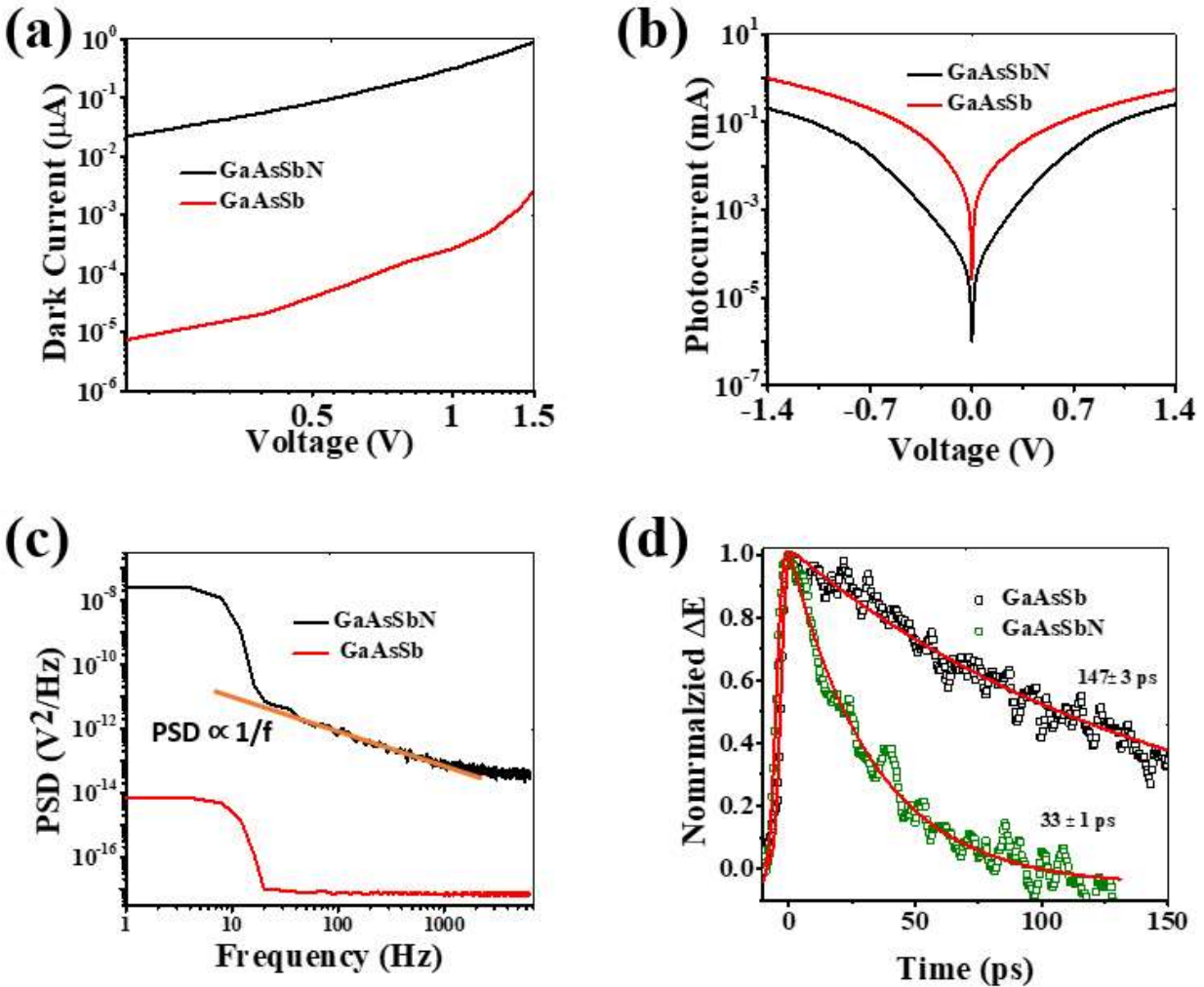


Figure: Electrical characterization of GaAsSb and GaAsSbN NW devices. Superimposed (a) dark current in a log-log scale. (b) photocurrent on a semilog scale. (c) low-frequency noise (LFN) data and $1/f$ trend line fit the GaAsSbN data under dark conditions, and (d) transient photoinduced change in the THz electric (E) field for GaAsSb and GaAsSbN NWs probed by OPTP spectroscopy. The solid lines represent a single exponential fit convoluted with a Gaussian function.

Contribution to other funded work

There has been cross-pollination from this work and the avalanche photodiode (APD) work funded by National Science Foundation (Award ECCS-1832117) growth optimization, doping assessment, band gap engineering, and response time measurements resulting in successful fabrication of both GaAsSb-based p-i-n NW based PDs and NWs based APD in both axial and C-S geometry. This work has also resulted in several journal publications, and support from this grant funding has been acknowledged. Associated journal publications and dissertations have been uploaded in the “Products” section.